Continuous flow conversion of biomass-derived methyl levulinate into gamma valerolactone using functional metal organic frameworks

Weiyi Ouyang [1,], Deyang Zhao[2], Yantao Wang [2], Alina M. Balu [1], Christophe Len [2,3], Rafael Luque [1,4] **

[1] Departamento de Química Orgánica, Universidad de Córdoba, Edif. Marie Curie, Ctra Nnal IV-A, Km 396, E14014, Córdoba, Spain. * E-mail: rafael.luque@uco.es

[2] Sorbonne Universités, Université de Technologie de Compiègne (UTC), CS 60319, 60203, Compiègne Cedex, France

[3] PSL Research University, Chimie Paris Tech, CNRS, Institut de Recherche de Chimie, Paris, 11 rue Pierre et Marie Curie, F-75231 Paris Cedex 05, France

[4]Peoples Friendship University of Russia (RUDN University), 6 Miklukho-Maklaya street, Moscow, 117198, Russia

ABSTRACT: Zirconium based metal organic framework, UiO-66 (Zr), was successfully synthesized via solvothermal method, followed by various characterization including XRD, thermal analysis, N_2 physisorption and TEM. As-synthesized UiO-66 (Zr) was employed in the transformation of methyl levulinate (ML) to gamma valerolactone (GVL) via catalytic transfer

hydrogenation (CTH) under continuous flow and various reaction conditions, which gave superior catalytic performance and efficiency as compared to reported catalysts. The obtained results show great potential of applying UiO-66 (Zr) in upgrading biomass derivatives to useful biofuel/chemical products, paving the way for green energy production from renewable resources.

Keywords: Biomass valorization, methyl levulinate, gamma valerolactone, continuous flow, catalytic transfer hydrogenation (CTH), metal organic framework, UiO-66 (Zr)

Introduction

Due to the limited reserve of fossil fuels and the rising awareness on sustainable development, low-carbon-economy has been proposed and is being implementing globally, which is urging the expansion of renewable and sustainable energy. In this regard, valorization of enormous and low-cost lignocellulosic biomass into biofuels and platform molecules is of vital importance and has attracted massive attention in the last few decades. A wide range of catalytic strategies have been developed for the transformation of lignocellulosic biomass into a wide range of chemicals, among which levulinic acid (LA) is listed as the top 12 prospective building blocks derived from sugars[1], indicating the great possibility in the valorization of levulinic acid and alkyl levulinates into valuable products. γ-valerolactone (GVL) is one of the promising platform molecule derived from lignocellulosic biomass via hydrogenation of levulinic acid and alkyl levulinates, which can be used as solvent, fuel additive and liquid fuel, as well as precursor for valuable chemicals (e.g. olefins, polymers, 5-nanonone).[2–5]

Catalysts, either homogeneous or heterogeneous, have key effects on the transformation of levulinic acid and its ester derivates to γ-valerolactone, including (supported) transition/noble

metals, metal hydroxides, metal oxides, metal salts.[6] A cobalt catalyst generated by reducing commercial Co_3O_4 was reported to be very efficient in solvent-free transformations of ethyl levulinate (EL) to GVL under mild condition.[7] $Ca_5(PO_4)_3(OH)$ (HAP) incorporated with metals (Pd, Pt, Ru, Cu, Ni) was employed in the vapor phase hydrogenation of levulinic acid, in which 2Ru/HAP catalyst gave most efficient GVL production with TOF_{GVL} of 2.9 s^{-1} as compared to catalysts decorated with other metals. Apart from metal catalysts, metal hydroxides such as $Ru(OH)_x/TiO_2$[8] and $Zr(OH)_4$ were also reported to be active in this transformation while giving good conversion and selectivity with excellent selectivity[9]. Considering the environmental impacts, metal hydroxides (homogeneous catalysts) are less preferable for separation/recycling issues while the high cost of noble metals will also limit their large-scale application in a certain content. In this aspect, metal oxides or supported metal oxides as catalysts offered an alternative to noble metal catalysts in the production GVL from LA or its esters in high yields such as ZrO_2[10,11], Cu/ZrO_2[12], $ZrFeO_x$[13], ZrO_2/SBA-15[14], SnO_2/SBA-15[15], etc.

Generally, there are two pathways for the catalytic hydrogenation upgrading of LA and its esters: (1) direct hydrogenation of the carbonyl group using molecular H_2; (2) catalytic transfer hydrogenation (CTH) of the carbonyl group using organic molecules (e.g., alcohols and formic acid) as hydrogen donors. Subsequently, the reaction intermediates will be transformed into GVL via intramolecular (trans)esterification. Due to the low solubility of molecular H_2 in most solvents, high H_2 pressure is essential to achieve high yields, which raises not only safety concerns but also hefty infrastructure cost at industrial scale. In contrast, organic molecules as hydrogen donors can be potentially promising alternatives to molecular H_2 with higher solubility in liquid phase reactions as well as easier controlling the degree in selective hydrogenation and/or hydrogenolysis.[16] CTH pathways using inexpensive organic molecules as hydrogen sources can

be safer, more feasible and cost-effective for the large scale GVL production. Especially, CTH processes using various alcohols (methanol, ethanol, isopropanol, etc.) as hydrogen donors to hydrogenate the carbonyl group via Meerwein–Ponndorf–Verley (MPV) reduction is attractive and widely reported in GVL production[4,11,15,17–19] because alcohols are low-cost and renewable hydrogen donors as well as solvents which can be separated from the reaction mixture and recycled into the feed.

Interestingly, zirconium based catalysts ($Zr(OH)_4$[9], ZrO_2[10,11], Cu/ZrO_2[12], $ZrFeO_x$[13], ZrO_2/SBA-15[14], Zr-beta[20], Zr-HPA[19], Al–Zr mixed oxides[17], etc.) have exhibited high catalytic activity and stability in the GVL production through CTH process due to their amphoteric properties which provide acid-base pair sites facilitating CTH via MPV reduction. Meanwhile, the recent emerging of metal organic frameworks (MOFs) have attracted intensive attention with widely application in various fields, including gas storage, separation, sensors, fuel cells, catalysis due to their excelling properties including large surface area, tunable structure, physicochemical properties and functionality of metal ions and organic ligands.[21–26] Applications of MOFs in upgrading lignocellulosic biomass and their derived platform molecules arise in recent year and show great potential for further development.[27] Similar to the aforementioned amphoteric catalysts, zirconium-based MOFs consisted of Zr oxo clusters and organic linkers can similarly function in CTH process. In this regard, MOF-808, UiO-66 (Zr) and its functionalized derivates were reported to be active in catalytic transfer hydrogenation of LA and its esters, achieving relatively high yield of GVL.[28,29] Zr^{4+}-O^{2-} acid-base pair sites located in the Zr oxo clusters are uniformly embedded in the porous framework with high surface area, boosting the reaction with efficient reagent diffusion as well as easy-accessible active sites. Moreover, the esterification reaction can also be benefited

from the Brönsted acidity of the μ_3-OH groups and organic linker defect sites[30–33], promoting the cyclization step in the GVL production.

However, the reported reactions with UiO-66 (Zr) were performed under batch conditions, while flow reactions are more preferable from the practical point of view due to its advantages (e.g. easy scale-up and purification, efficient energy utilization).[34]

In the present work, we demonstrated the application of UiO-66 (Zr) in GVL production via CTH of ML in continuous flow under various reaction conditions. ML was selected as precursor in this work since acid-free alkyl levulinates produced by alcoholysis of various carbohydrates has low boiling point which are easier in production and separation as compared to LA.[10,35,36]

Experimental

Materials

$ZrCl_4$ (>99.5%, Sigma-Aldrich), terephthalic acid (>99%, Acros), isopropanol (>99.9%, PanReac), GVL (>99%, Sigma-Aldrich), decane (>99%, Acros), HCl (37%, Sigma-Aldrich), dimethylformamide (>99.9%, PanReac), methanol (>99.9%, PanReac), ethanol (>99.9%, PanReac) were employed as purchased. ML (>99.5%) was provided by Avantium Chemicals BV as side product from the YXY process after purification.

Synthesis of UiO-66 (Zr)

In a typical procedure, a mixture of $ZrCl_4$ (2000 mg, 8.54 mmol) and 16 mL concentrated (37%) HCl were first added to 80 mL DMF and sonicated for 20 min. Thereafter, terephthalic acid (2000 mg, 12 mmol) and 80 mL DMF were added to the above mixture and sonicated for another 20

min. Then the mixture was transferred to a 500 mL teflon bottle and heated at 120 °C for 24 h in an oven. The generated precipitates were separated by filtration, washed first with DMF (100 mL x 2 x 30 min) and then with methanol (100 mL x 2 x 30 min), and then dried naturally and activated under vacuum at 80 °C.

Material characterization

Powder diffraction patterns were recorded in a Bruker D8 DISCOVER A25 diffractometer using Ni filtered Cu Kα (λ = 1.5418 Å) radiation and operated at 40 KeV and 40 mA. N_2 physisorption isotherms were measured at 77 K using a Micromeritics ASAP 2020 automated system to understand the textural properties of the samples. Samples were degassed under vacuum (0.1 Pa) for overnight at 423 K prior to the measurement. Thermal gravimetric analysis of the catalysts was performed with simultaneous TG-DTA measurement in System Setaram Setsys 12 TGA instrument. The analysis started at 30 ^{o}C with a ramping rate of 10 ^{o}C/min till 800 ^{o}C in air atmosphere (50 mL/min). Transmission electron microscopy (TEM) images were recorded by Jeol JEM 2010 with resolution of 0.38 nm at the Research Support Service Center (SCAI) from Universidad de Cordoba.

Continuous catalytic transfer hydrogenation of ML

The catalytic transfer hydrogenation of ML was carried out in the continuous flow reactor, Phoenix, from ThalesNano Inc. In detail, 0.23 g catalysts were packed in the catalyst cartridge with cotton filled on both sides to avoid blockage. Different amounts of ML were diluted in isopropanol to obtain the desired concentration with decane as internal standard. Reaction conditions were optimized by varying different reaction parameters, such as temperature, pressure,

concentration, flowrate. Solvent effect was also investigated by changing isopropanol to other alcohols. Blank experiment was performed without packing catalysts in the cartridge. Samples were collected on specific time-on-stream.

Analysis of liquid samples

The collected samples were analyzed by gas-chromatography (Agilent 5890 Series II) equipped with FID detector and SUPELCO EQUITY TM-1 fused silica capillary column (60 m × 0.25 mm × 0.25 μm). The injector and detector temperatures were set as 250 ºC. The oven temperature was held for 1 minute at 60 ºC, and then increased to 230 ºC in 17 minutes and held for 5 minutes. Products analysis was carried out in GC-MS equipped with HP-5 column from SCAI of Universidad de Cordoba, using the same temperature setting as previous description. Conversion, selectivity and GVL productivity were calculated as below:

$$Conversion = \frac{(C_{ML,initial} - C_{ML,final})}{C_{ML,initial}} \times 100\% \quad (1)$$

$$Selectivity = \frac{C_{GVL}}{C_{ML,initial} - C_{ML,final}} \times 100\% \quad (2)$$

$$Productivity = \frac{hourly\ molar\ flow\ rate\ of\ GVL}{m_{catalyst}} \quad (3)$$

where C represents molar concentration and m represents weight.

Results and discussion

Catalytic transformation of ML to GVL over UiO-66 (Zr)

Optimization of key reaction parameters

According to previous reports, reaction temperature plays a key role in the CTH of alkyl levulinates.[10,28,29] Reaction temperatures were firstly optimized by varying from 180 ºC to 240 ºC while controlling the other parameters as below: 0.6 mol/L ML in isopropanol, flowrate = 0.3 mL/min, 35 bar, 0.23 g UiO-66. The results are illustrated in **Figure 1**, which shows that the higher reaction temperature favors the transformation of ML to GVL. In detail, the main by-products are the transesterification product – isopropyl levulinate and slight amount of reaction intermediate – methyl 4-hydroxypentanoate. It can be seen from **Figure 1** that there is strong competence between CTH pathway and transesterification pathway at lower temperature, while higher temperature promotes CTH pathway. Therefore, ML conversion was slightly improved within the investigated temperature range, while GVL selectivity was greatly improved from 49% to 96%. As a result, GVL productivity is then increased along at increasing conversion and selectivity. Meanwhile, it also indicates that the processing ability of UiO-66 (Zr) is boosted by an increase in reaction temperature. ML conversion and GVL selectivity reached >99% and 96% at the optimum temperature, 240 ºC, respectively, with the productivity of 29.9 $mmol_{GVL}g^{-1}h^{-1}$. Reaction temperature was subsequently set as 240 ºC in the following experiments.

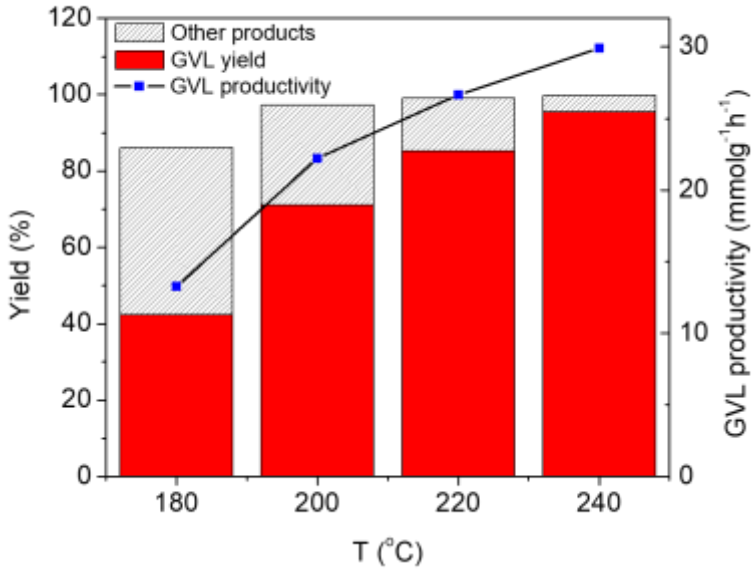

Figure 1. Catalytic performance of UiO-66 (Zr) in CTH of ML under different temperatures. Reaction conditions: 0.23 g UiO-66 (Zr), 0.6 mol/L ML in isopropanol, flowrate = 0.3 mL/min, 35 bar. Time-on-stream (TOS) = 1 hour.

Both the effects of reagent flowrates and ML concentration on the reaction were subsequently investigated under the previous optimized temperature (240 ºC). The flowrate was varied from 0.1 to 0.4 mL/min while maintaining ML concentration of 0.6 M. As seen in **Figure 2** (a), ML conversion and the GVL selectivity remained almost unchanged under the investigated reaction conditions, giving higher GVL productivity with an increase in ML flowrate (molar flux). For better understanding the effect of ML molar flux, ML flowrate and concentration were varied to maintain the same ML molar flux, with results summarized in **Figure 2** (b). The catalytic performance of UiO-66 (Zr) did not change with the same ML molar flux though the ML flowrate and concentration were different, giving the same GVL productivity with both conversion and selectivity over 90%. ML flowrate and concentration are not independent factors influencing the catalytic performance, while ML molar flux is the essential factor. In practical point of view, when

giving the same catalytic performance, process with lower flowrate and higher concentration is preferable that costs less in the separation step. 57.5 $mmol_{GVL}g^{-1}h^{-1}$ GVL productivity, with ML conversion over 99% and GVL selectivity of 93%, was achieved under the following reaction conditions: 2.4 M ML in isopropanol, flowrate = 0.1 mL/min, 240 ºC, 35 bar, 0.23 g UiO-66 (Zr). Due to the excellent conversion and selectivity, the flowrate was doubled for better understanding the catalytic ability of UiO-66 (Zr). In this regard, ML conversion decreased from over 99% to 83.1% with slight drop in GVL selectivity (from 93% to 89), while the GVL productivity was dramatically enhanced by 160% (from 57.5 to 92.3 $mmol_{GVL}g^{-1}h^{-1}$). Considering the reusability of the reagent and solvent, the improvement in efficiency compensates the slight drop in terms of conversion and selectivity. Hence, ML concentration and flowrate was set as 2.4 M and 0.2 mL/min, respectively, in the following experiments.

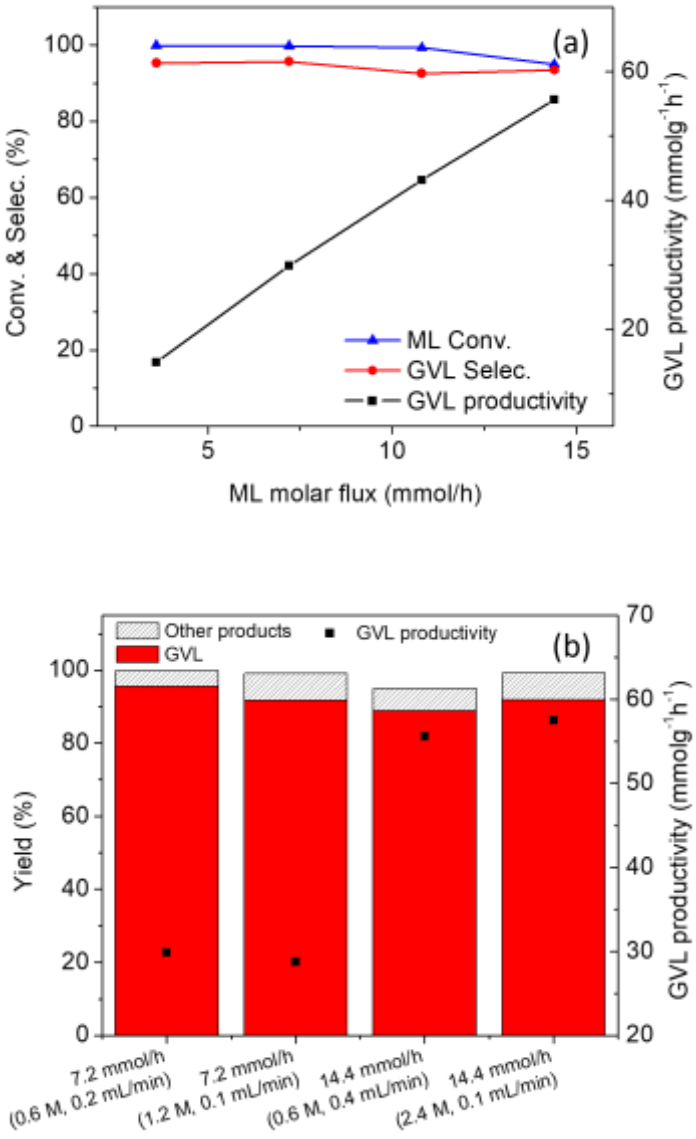

Figure 2. Effect of ML molar flux on the catalytic performance of UiO-66 (Zr) in CTH of ML. Reaction conditions: 0.23 g UiO-66 (Zr), 240 ºC, 35 bar. (a: 0.6 M ML in isopropanol). Time-on-stream (TOS) = 1 hour.

The effect of reaction pressure was studied with variation from 0 to 50 bar (in the back-pressure regulator) with previous optimized temperature, concentration and flowrate, which results are

illustrated in **Figure 3**. The catalytic transformation of ML rarely proceeds without the addition of system pressure, while it is greatly improved in the presence of pressure. In detail, ML conversion increased from 10% to 85% by applying 20 bar system pressure, and further increase of pressure to 35 bar didn't have obvious effect on conversion while promoting the GVL selectivity from 63% to 89%. When increasing the pressure to 50 bar, only ML conversion was slightly increased (ca. 10%). It can be concluded that the increase of pressure favors the CTH of ML to GVL in terms of both conversion and selectivity, resulting in higher GVL productivity. This improvement could be attributed to the enhancement of reagents' adsorption on the catalyst surface, facilitating the contact between reagents and the catalytic sites

Finally, the solvent effect was also studied by changing isopropanol to methanol and ethanol. Nearly no ML conversion was observed when using methanol as hydrogen donor and solvent. Though the reaction achieved 89% ML conversion in case of using ethanol, more by-products was yielded (mainly the transesterification product, ethyl levulinate) that only 37% GVL yield was obtained. The lower catalytic activity could be attributed to the higher reduction potential of methanol and ethanol than that of isopropanol.[9,13]

Above all, optimized reaction condition in the conversion of ML to GVL are as follows: 0.23 g UiO-66 (Zr), 2.4 M ML in isopropanol, flowrate = 0.2 mL/min, 240 ^{o}C, 35 bar, which were applied to test the stability of the UiO-66 (Zr).

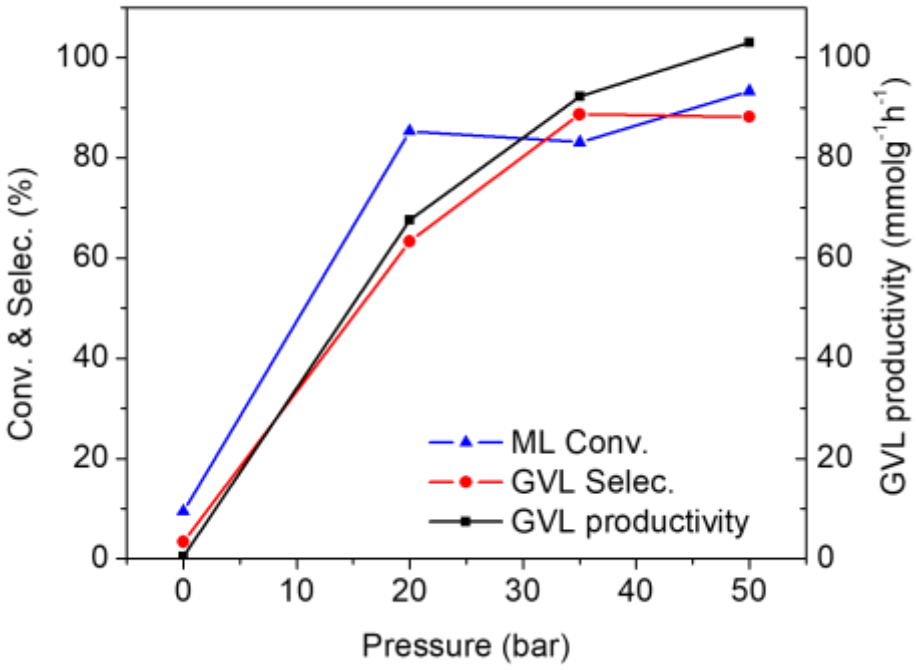

Figure 3. Effect of reaction pressure on the catalytic transformation of ML using UiO-66 (Zr). Reaction conditions: 0.23 g UiO-66 (Zr), 2.4 M ML in isopropanol, flowrate = 0.2 mL/min, 240ºC. Time-on-stream (TOS) = 1 hour.

Long term stability

For better understanding the stability of UiO-66 (Zr), the reaction was performed under the previous optimized reaction conditions with longer time-on-stream. The result illustrated in **Figure 4** shows that the catalytic activity of UiO-66 (Zr) was quite stable in the first 9 hours on stream, with only slight decrease of ML conversion. With the continuation of the reaction, ML conversion slowly decreased to 56 % at the end with TOS = 30 hours, giving the GVL productivity of 58.94 $mmol_{GVL}g^{-1}h^{-1}$, while the GVL selectivity was well preserved over the whole experiment. The drop of conversion can be attributed to the catalyst deactivation along the reaction that small amount of di-isopropyl terephthalate was detected by GC-MS analysis of the collected samples, which is

consistent with the TGA curves in **Figure 6** that UiO-66 (Zr) was converted into amorphous zirconia-via $Zr(OH)_4$-after the reaction because of loss of organic ligands. Loss organic ligand was also reported in the same reaction by the other researchers, which loss one organic linker per unit formula after 5 cycles reaction.[28]

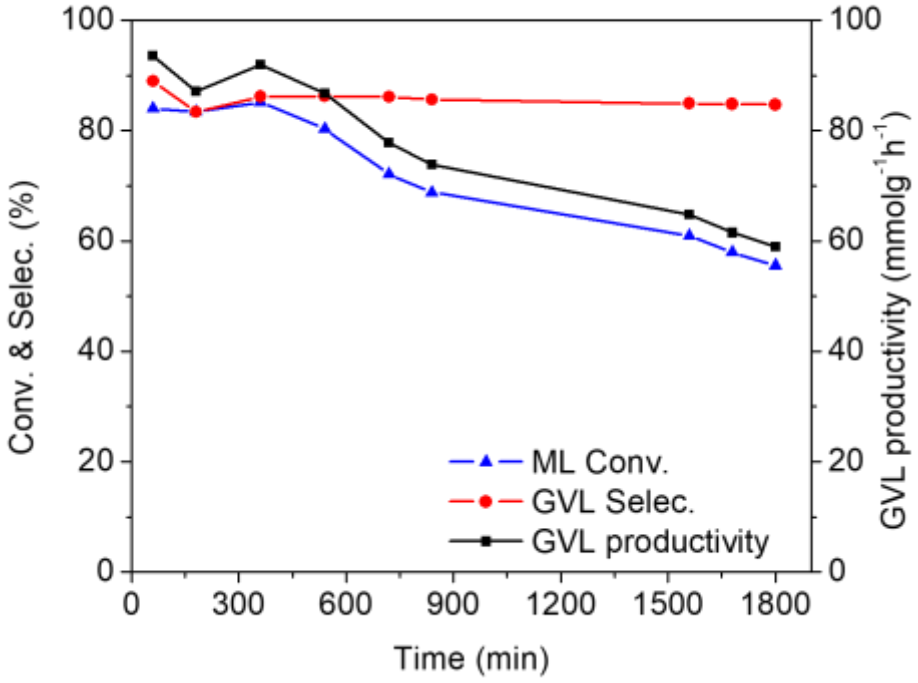

Figure 4. Long term stability of UiO-66 (Zr) in catalytic transformation of ML to GVL. Reaction conditions: 0.23 g UiO-66 (Zr), 2.4 M ML in isopropanol, flowrate = 0.2 mL/min, 240 ºC, 35 bar.

Comparison of catalytic performance between UiO-66 (Zr) and literature

The catalytic performance of UiO-66 (Zr) was compared with the literature values, which is summarized in **Table 1**. The optimal GVL productivity in the present work is 92.3 $mmol_{GVL}g^{-1}h^{-1}$ (TOS = 1 h), while it decreases to 58.9 $mmol_{GVL}g^{-1}h^{-1}$ after 30 hours on streaming, which is still much higher than those reported values (c.a. 1 $mmol_{GVL}g^{-1}h^{-1}$) obtained in batch using UiO-66 (Zr)

and its derivates as catalysts. Though 39.2 $mmol_{GVL}g^{-1}h^{-1}$ GVL productivity was achieved using ZrFeO(1:1)-300 as catalysts, it is still much lower than that obtained in this work. Therefore, excellent catalytic performance of UiO-66 (Zr) was obtained under the investigated reaction conditions, which is superior to the reported values.

Table 1. Comparison of catalytic performance between UiO-66 (Zr) and literature

Entry	Catalyst	Conditions	Conv. (%)	Selec. (%)	GVL productivity ($mmol \cdot g^{-1} \cdot h^{-1}$)	Ref.
1	UiO-66 (Zr)	0.23 g catalysts, 2.4 M ML in isopropanol, flowrate = 0.2 mL/min, 240 °C, 35 bar, TOS = 1 h	83	89	92.3	This work
2	UiO-66 (Zr) deactivated	0.23 g catalysts, 2.4 M ML in isopropanol, flowrate = 0.2 mL/min, 240 °C, 35 bar, TOS = 30 h	56	85	58.9	
3	UiO-66 (Zr)	0.22 g catalysts, 4 mmol ethyl levulinate in 400 mmol isopropanol, 130 °C, t = 3 h (batch reaction)	43.3	18.5	0.534	[28]
4	MOF-808		100	85	5.66	
5	UiO-66 (Zr)	0.1 g catalysts, 1 mmol ML in 5 mL 2-butanol, 140 °C, Ar 0.5 MPa, t = 9 h (batch reaction)	70	51	0.4	[29]
6	UiO-66-S_{60}		98	82	0.889	
7	UiO-66-S_{60}[a]	0.1 g catalysts, 1 mmol ML in 5 mL 2-butanol, 180 °C, Ar 0.5 MPa, t = 9 h (batch reaction)	>99.5	93	1.03	
8	Al_7Zr_3-300[b]	0.072g catalysts, 1 mmol ethyl levulinate in 5 mL isopropanol, 220 °C, t = 4 h (batch reaction)	95.5	87.1	2.89	[17]

9	$Zr(OH)_4$	1 g catalysts, 2g ethyl levulinate in 38 g ethanol, 240 ºC, t = 1 h (batch reaction)	89.1	84.5	10.7	[9]
10	ZrFeO(1:1)-300[c]	0.2 g catalysts, 0.65 g ethyl levulinate in 11.8 g isopropanol, 230 ºC, t = 0.5 h (batch reaction)	94.2	92	39.2	[13]
11	ZrFeO(1:3)-300[d]	0.2 g catalysts, 0.65 g ethyl levulinate in 11.8 g ethanol, 230 ºC, t = 3 h (batch reaction)	93.3	93.5	7.51	

[a] S_{60} represents 60 mol% sulfonated ligand

[b] molar ratio Al:Zr = 7:3; the sample was calcined at 300 ºC

[c] molar ratio Zr:Fe = 1:1; the sample was calcined at 300 ºC

[d] molar ratio Zr:Fe = 1:3; the sample was calcined at 300 ºC

Material characterization

Powder XRD analysis was carried to understand the crystal structure of the as-synthesized sample. The peaks at $2\theta = 7.43^o$ and 8.58^o presence in the obtained XRD pattern (**Figure 5**, a) are two characteristic peaks of UiO-66 (Zr), which can be ascribed to the (111) and (002) planes respectively, confirming the consistent crystalline structure of the sample with the literature.[37]. Besides, no obvious peak of impurities was observed, indicating the high purity of the sample. However, no peak was observed for the sample recovered from the long-term stability tests, indicating that the crystallinity was not preserved after reaction, derived from the continuous loss of the organic ligand during the reaction. N_2 absorption-desorption isotherm (**Figure 5Figure 5**, b) of UiO-66 (Zr) exhibited typical type I isotherm with sharp increase at low pressure (P/P_0 <

0.1), characteristic of microporous materials. BET surface area of the as-synthesized UiO-66 (Zr) is 1147 m^2/g while its total pore volume is 0.58 cm^3/g. The BET surface area decreased to 109 m^2/g after the long-term stability test, which could be ascribed to the structure collapsion resulted from the loss of organics ligands.

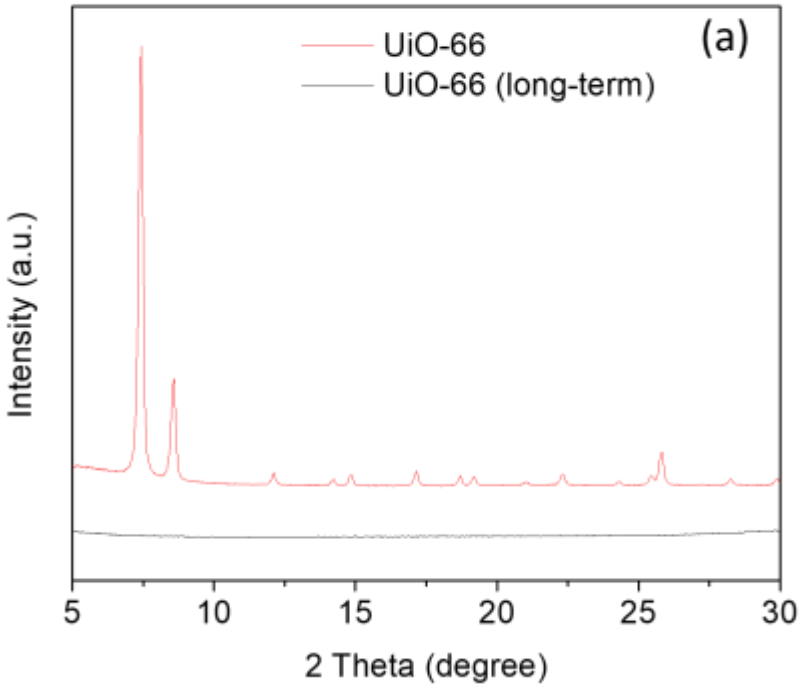

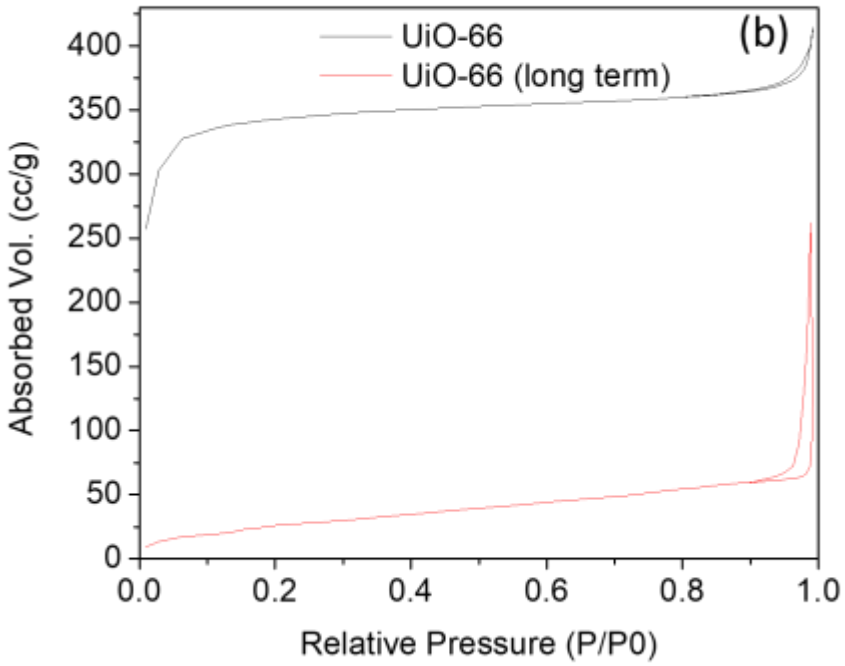

Figure 5. XRD pattern (a) and N_2 absorption-desorption isotherm (b) of fresh UiO-66 (Zr) and UiO-66 (Zr) after long-term stability test

TGA curves of fresh UiO-66 (Zr) and used UiO-66 (Zr) in long-term stability test were illustrated in **Figure 6**. For fresh UiO-66 (Zr), the weight loss at temperature lower than 100 ºC was attributed to loss of physisorbed water. Subsequently, progressive weight loss was observed until 300 ºC, resulting from DMF removal and the dehydration of $Zr_6O_4(OH)_4$ nodes to Zr_6O_6, in good agreement with previous reports in which the MOF formula after dehydration was proposed to be $Zr_6O_{6+x}BDC_{6-x}$, where x stands for the missing ligands (from the synthetic protocol).[33,37,38]

Last, the weight dropped sharply at ca. 500 ºC because of the decomposition of the organic linkers, with a 42.8% weight remaining after the thermal treatment to 800ºC (TGA analysis was performed in air atmosphere). The decomposition of four organic linkers (4BDC, Figure 6) is responsible of the observed mass loss in the 350-600ºC region (33.6%) based on the literature reported MOF

formula. These results are in good agreement with previous literature reports in which as-synthesized UiO-66 (Zr) containing only 4 linkers per formula unit were synthesized in HCl medium[38]. The reported findings herein also pointed out a highly defective structure in our UiO-66 (Zr), with potential benefits in catalytic reactions promoted by Brönsted acidic sites[30,31,39]. Nevertheless, UiO-66 (Zr) was finally decomposed into ZrO_2 (via $Zr(OH)_4$) as confirmed from TGA experiments[40] and XRD data (results not shown) due to the continuous loss of organic ligands during reaction under the investigated moderate temperatures (180-240ºC) and continuous flow conditions.

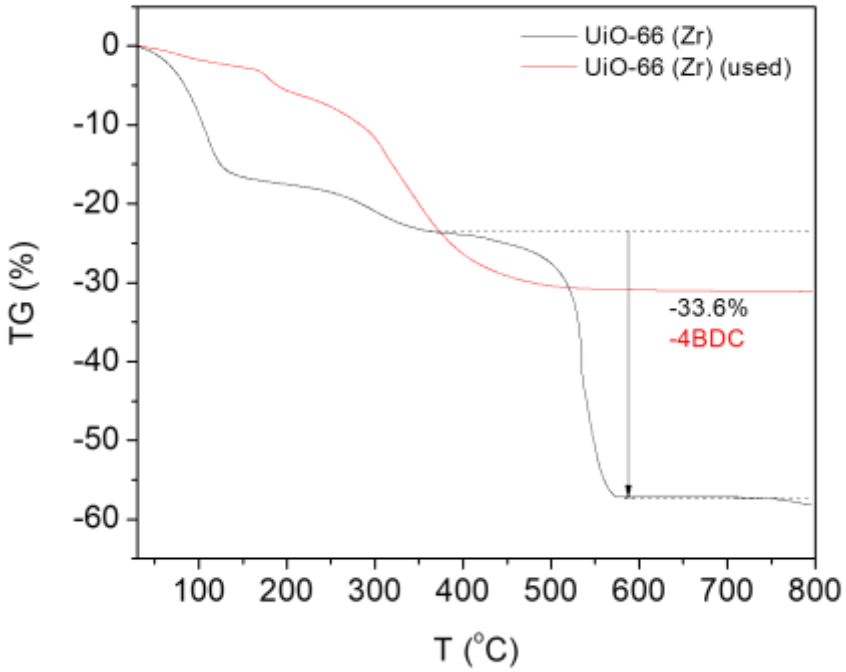

Figure 6 TGA curve of fresh UiO-66 (Zr) and UiO-66 (Zr) after long-term stability test

TEM images of fresh and used UiO-66 (Zr) are shown in **Figure 7**. The surface of fresh UiO-66 (Zr) turned from smooth into rough after the long-term stability test, which could be ascribed to

the loss of organic linkers during reaction and the formation of an amorphous ZrO_2 phase. The loss of organic linkers eventually leads to a collapse of the UiO-66 (Zr) structure and was found to have a detrimental effect in catalytic performance.

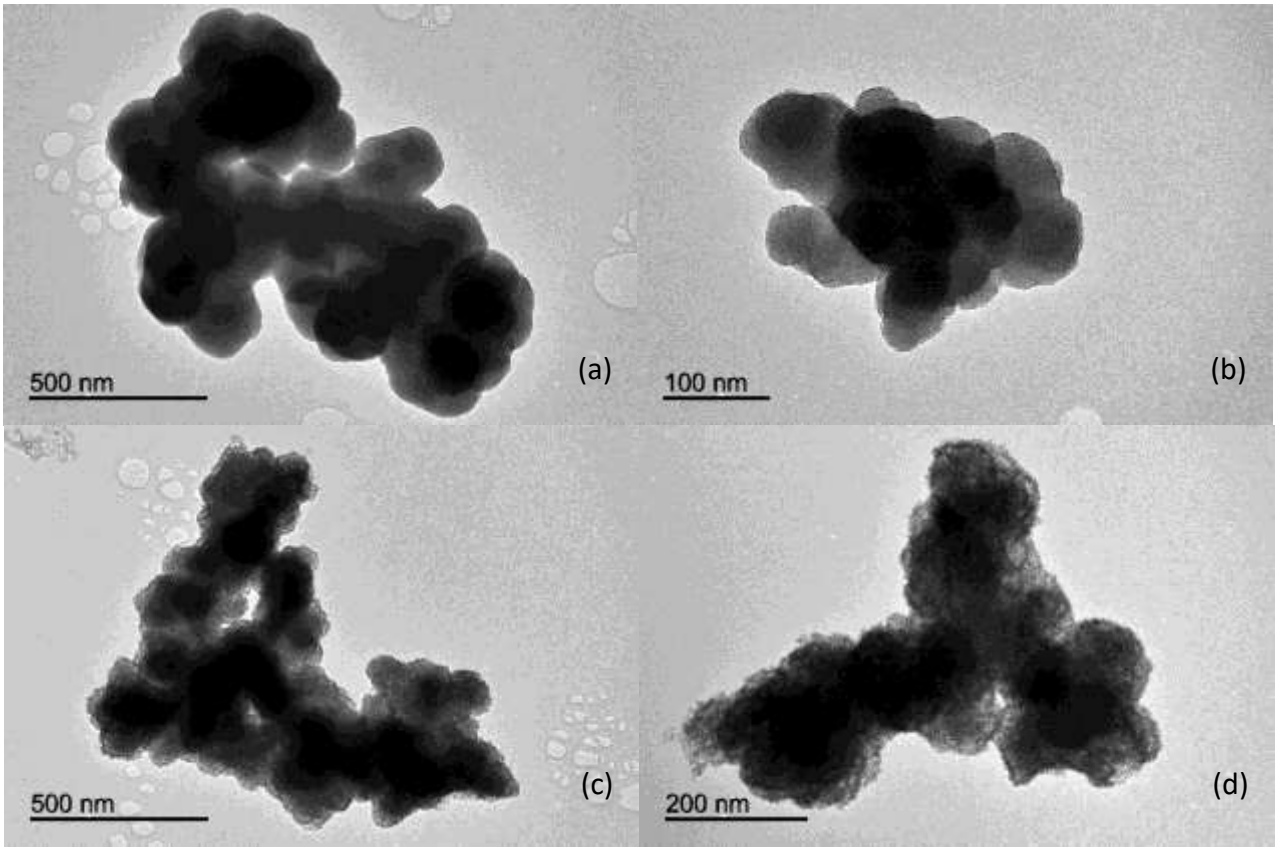

Figure 7 TEM images of fresh UiO-66 (Zr) (a, b) and UiO-66 (Zr) after long-term stability test (c, d)

Conclusions

Defective UiO-66 (Zr) with 4 linkers per formula unit was successfully synthesized in the present work and subsequently employed in the catalytic transformation of ML into GVL via CTH process, giving out excellent GVL productivity as compared to literature results. Slight loss of organic

linkers was observed during the reaction, which resulted in a gradual crystallinity loss and composition of UiO-66 (Zr) eventually deriving into the formation of an amorphous zirconia phase. Since the ML used in the present work was obtained as by-product from the YXY process of Avantium Chemicals BV, there is great potential in the application of efficient UiO-66 (Zr) in the continuous production of GVL, as well as other processes. Further research is still necessary to investigate the possibility to fully preserve the structure of UiO-66 (Zr) under continuous flow at moderate to high temperatures (>200ºC).

Acknowledgements

Rafael Luque gratefully acknowledges funding from the European Union's Horizon 2020 research and innovation programme under the Marie Sklodowska-Curie grant agreement No 641861 (especially for funding W. Ouyang's Ph.D studies) as well as funding from MINECO under project CTQ2016-78289-P, co-financed with FEDER funds. The authors gratefully acknowledge the financial support from the European COST Action FP1306 for an STSM granted to Y. Wang. D. Zhao and Y. Wang thanks the China Scholarship Council for financial support. The publication has been prepared with support of RUDN University Program 5-100.

Abbreviations

BET	Brunauer–Emmett–Teller
CTH	catalytic transfer hydrogenation
EL	ethyl levulinate
GVL	γ-valerolactone

LA	levulinic acid
ML	methyl levulinate
MOFs	metal organic frameworks
MPV	Meerwein–Ponndorf–Verley
TEM	transmission electronic microscopy
TOF	turn-over-frequency
TOS	time-on-stream
XRD	X-ray diffraction

References

(1) Werpy, T.; Petersen, G. *Top Value Added Chemicals from Biomass: Volume I -- Results of Screening for Potential Candidates from Sugars and Synthesis Gas*; Golden, CO, 2004. DOI: 10.2172/15008859

(2) Alonso, D. M.; Wettstein, S. G.; Dumesic, J. A. Gamma-valerolactone, a sustainable platform molecule derived from lignocellulosic biomass. *Green Chem.* **2013**, *15* (3), 584–595. DOI: 10.1039/c3gc37065h

(3) Serrano-Ruiz, J. C.; Wang, D.; Dumesic, J. a. Catalytic upgrading of levulinic acid to 5-nonanone. *Green Chem.* **2010**, *12* (4), 574–577. DOI: 10.1039/b923907c

(4) Kuwahara, Y.; Kaburagi, W.; Osada, Y.; Fujitani, T.; Yamashita, H. Catalytic transfer

hydrogenation of biomass-derived levulinic acid and its esters to γ-valerolactone over ZrO_2 catalyst supported on SBA-15 silica. *Catal. Today* **2017**, *281*, 418–428. DOI: 10.1016/j.cattod.2016.05.016

(5) Wang, D.; Hakim, S. H.; Martin Alonso, D.; Dumesic, J. A. A highly selective route to linear alpha olefins from biomass-derived lactones and unsaturated acids. *Chem. Commun.* **2013**, *49* (63), 7040--7042. DOI: 10.1039/c3cc43587c

(6) Liguori, F.; Moreno-Marrodan, C.; Barbaro, P. Environmentally Friendly Synthesis of γ-Valerolactone by Direct Catalytic Conversion of Renewable Sources. *ACS Catal.* **2015**, *5* (3), 1882–1894. DOI: 10.1021/cs501922e

(7) Zhou, H.; Song, J.; Fan, H.; Zhang, B.; Yang, Y.; Hu, J.; Zhu, Q.; Han, B. Cobalt catalysts: very efficient for hydrogenation of biomass-derived ethyl levulinate to gamma-valerolactone under mild conditions. *Green Chem.* **2014**, *16* (8), 3870–3875. DOI: 10.1039/C4GC00482E

(8) Kuwahara, Y.; Kaburagi, W.; Fujitani, T. Catalytic transfer hydrogenation of levulinate esters to γ-valerolactone over supported ruthenium hydroxide catalysts. *RSC Adv.* **2014**, *4* (86), 45848–45855. DOI: 10.1039/C4RA08074B

(9) Tang, X.; Chen, H.; Hu, L.; Hao, W.; Sun, Y.; Zeng, X.; Lin, L.; Liu, S. Conversion of biomass to γ-valerolactone by catalytic transfer hydrogenation of ethyl levulinate over metal hydroxides. *Appl. Catal. B Environ.* **2014**, *147*, 827–834. DOI: 10.1016/j.apcatb.2013.10.021

(10) Tang, X.; Hu, L.; Sun, Y.; Zhao, G.; Hao, W.; Lin, L. Conversion of biomass-derived ethyl

levulinate into γ-valerolactone via hydrogen transfer from supercritical ethanol over a ZrO_2 catalyst. *RSC Adv.* **2013**, *3* (26), 10277–10284. DOI: 10.1039/c3ra41288a

(11) Chia, M.; Dumesic, J. A. Liquid-phase catalytic transfer hydrogenation and cyclization of levulinic acid and its esters to γ-valerolactone over metal oxide catalysts. *Chem. Commun.* **2011**, *47* (44), 12233–12235. DOI: 10.1039/c1cc14748j

(12) Hengne, A. M.; Rode, C. V. Cu–ZrO_2 nanocomposite catalyst for selective hydrogenation of levulinic acid and its ester to γ-valerolactone. *Green Chem.* **2012**, *14* (4), 1064–1072. DOI: 10.1039/c2gc16558a

(13) Li, H.; Fang, Z.; Yang, S. Direct Conversion of Sugars and Ethyl Levulinate into γ-Valerolactone with Superparamagnetic Acid–Base Bifunctional $ZrFeO_x$ Nanocatalysts. *ACS Sustain. Chem. Eng.* **2016**, *4* (1), 236–246. DOI: 10.1021/acssuschemeng.5b01480

(14) Enumula, S. S.; Gurram, V. R. B.; Kondeboina, M.; Burri, D. R.; Kamaraju, S. R. R. ZrO_2 /SBA-15 as an efficient catalyst for the production of γ-valerolactone from biomass-derived levulinic acid in the vapour phase at atmospheric pressure. *RSC Adv.* **2016**, *6* (24), 20230–20239. DOI: 10.1039/C5RA27513J

(15) Xu, S.; Yu, D.; Ye, T.; Tian, P. Catalytic transfer hydrogenation of levulinic acid to γ-valerolactone over a bifunctional tin catalyst. *RSC Adv.* **2017**, *7* (2), 1026–1031. DOI: 10.1039/C6RA25594A

(16) Gilkey, M. J.; Xu, B. Heterogeneous Catalytic Transfer Hydrogenation as an Effective Pathway in Biomass Upgrading. *ACS Catal.* **2016**, *6* (3), 1420–1436. DOI: 10.1021/acscatal.5b02171

(17) He, J.; Li, H.; Lu, Y.; Liu, Y.; Wu, Z.; Hu, D.; Yang, S. Cascade catalytic transfer hydrogenation–cyclization of ethyl levulinate to γ -valerolactone with Al–Zr mixed oxides. *Appl. Catal. A Gen.* **2016**, *510*, 11–19. DOI: 10.1016/j.apcata.2015.10.049

(18) Yang, Z.; Huang, Y.-B.; Guo, Q.-X.; Fu, Y. RANEY® Ni catalyzed transfer hydrogenation of levulinate esters to γ-valerolactone at room temperature. *Chem. Commun.* **2013**, *49* (46), 5328–5330. DOI: 10.1039/c3cc40980e

(19) Song, J.; Wu, L.; Zhou, B.; Zhou, H.; Fan, H.; Yang, Y.; Meng, Q.; Han, B. A new porous Zr-containing catalyst with a phenate group: an efficient catalyst for the catalytic transfer hydrogenation of ethyl levulinate to γ-valerolactone. *Green Chem.* **2015**, *17* (3), 1626–1632. DOI: 10.1039/C4GC02104E

(20) Wang, J.; Jaenicke, S.; Chuah, G.-K. Zirconium–Beta zeolite as a robust catalyst for the transformation of levulinic acid to γ-valerolactone via Meerwein–Ponndorf–Verley reduction. *RSC Adv.* **2014**, *4* (26), 13481–13489. DOI: 10.1039/C4RA01120A

(21) Li, J. R.; Sculley, J.; Zhou, H. C. Metal-organic frameworks for separations. *Chem. Rev.* **2012**, *112* (2), 869–932. DOI: 10.1021/cr200190s

(22) Kreno, L. E.; Leong, K.; Farha, O. K.; Allendorf, M.; Van Duyne, R. P.; Hupp, J. T. Metal–Organic Framework Materials as Chemical Sensors. *Chem. Rev.* **2012**, *112* (2), 1105–1125. DOI: 10.1021/cr200324t

(23) Dhakshinamoorthy, A.; Asiri, A. M.; Garcia, H. Mixed-metal or mixed-linker metal organic frameworks as heterogeneous catalysts. *Catal. Sci. Technol.* **2016**, *6* (14), 5238–5261. DOI: 10.1039/C6CY00695G

(24) Zhao, M.; Yuan, K.; Wang, Y.; Li, G.; Guo, J.; Gu, L.; Hu, W.; Zhao, H.; Tang, Z. Metal–organic frameworks as selectivity regulators for hydrogenation reactions. *Nature* **2016**, *539* (7627), 76–80. DOI: 10.1038/nature19763

(25) Zou, L.; Feng, D.; Liu, T.-F.; Chen, Y.-P.; Yuan, S.; Wang, K.; Wang, X.; Fordham, S.; Zhou, H.-C. A versatile synthetic route for the preparation of titanium metal–organic frameworks. *Chem. Sci.* **2016**, *7* (2), 1063–1069. DOI: 10.1039/C5SC03620H

(26) Furukawa, H.; Cordova, K. E.; O'Keeffe, M.; Yaghi, O. M. The Chemistry and Applications of Metal-Organic Frameworks. *Science (80-.).* **2013**, *341* (6149), 1230444–1230444. DOI: 10.1126/science.1230444

(27) Herbst, A.; Janiak, C. MOF catalysts in biomass upgrading towards value-added fine chemicals. *CrystEngComm* **2017**, *19* (29), 4092–4117. DOI: 10.1039/C6CE01782G

(28) Valekar, A. H.; Cho, K.-H.; Chitale, S. K.; Hong, D.-Y.; Cha, G.-Y.; Lee, U.-H.; Hwang, D. W.; Serre, C.; Chang, J.-S.; Hwang, Y. K. Catalytic transfer hydrogenation of ethyl levulinate to γ-valerolactone over zirconium-based metal–organic frameworks. *Green Chem.* **2016**, *18* (16), 4542–4552. 10.1039/C6GC00524A

(29) Kuwahara, Y.; Kango, H.; Yamashita, H. Catalytic Transfer Hydrogenation of Biomass-Derived Levulinic Acid and Its Esters to γ-Valerolactone over Sulfonic Acid-Functionalized UiO-66. *ACS Sustain. Chem. Eng.* **2017**, *5* (1), 1141–1152. DOI: 10.1021/acssuschemeng.6b02464

(30) Klet, R. C.; Liu, Y.; Wang, T. C.; Hupp, J. T.; Farha, O. K. Evaluation of Brønsted acidity and proton topology in Zr- and Hf-based metal–organic frameworks using potentiometric

acid–base titration. *J. Mater. Chem. A* **2016**, *4* (4), 1479–1485. DOI: 10.1039/C5TA07687K

(31) Ling, S.; Slater, B. Dynamic acidity in defective UiO-66. *Chem. Sci.* **2016**, *7* (7), 4706–4712. DOI: 10.1039/C5SC04953A

(32) Cirujano, F. G.; Corma, A.; Llabrés I Xamena, F. X. Zirconium-containing metal organic frameworks as solid acid catalysts for the esterification of free fatty acids: Synthesis of biodiesel and other compounds of interest. *Catal. Today* **2015**, *257* (Part 2), 213–220. DOI: 10.1016/j.cattod.2014.08.015

(33) Trickett, C. A.; Gagnon, K. J.; Lee, S.; Gándara, F.; Bürgi, H. B.; Yaghi, O. M. Definitive Molecular Level Characterization of Defects in UiO-66 Crystals. *Angew. Chemie - Int. Ed.* **2015**, *54* (38), 11162–11167. DOI: 10.1002/anie.201505461

(34) Wegner, J.; Ceylan, S.; Kirschning, A. Ten key issues in modern flow chemistry. *Chem. Commun.*. **2011**, *47* (16), 4583–4592. DOI: 10.1039/c0cc05060a

(35) Yu, F.; Zhong, R.; Chong, H.; Smet, M.; Dehaen, W.; Sels, B. F. Fast catalytic conversion of recalcitrant cellulose into alkyl levulinates and levulinic acid in the presence of soluble and recoverable sulfonated hyperbranched poly(arylene oxindole)s. *Green Chem.* **2017**, *19* (1), 153–163. DOI: 10.1039/C6GC02130A

(36) Peng, L.; Lin, L.; Li, H.; Yang, Q. Conversion of carbohydrates biomass into levulinate esters using heterogeneous catalysts. *Appl. Energy* **2011**, *88* (12), 4590–4596. DOI: 10.1016/j.apenergy.2011.05.049

(37) Cavka, J. H.; Jakobsen, S.; Olsbye, U.; Guillou, N.; Lamberti, C.; Bordiga, S.; Lillerud, K.

P. A New Zirconium Inorganic Building Brick Forming Metal Organic Frameworks with Exceptional Stability. *J. Am. Chem. Soc.* **2008**, *130* (42), 13850–13851. DOI: 10.1021/ja8057953

(38) Katz, M. J.; Brown, Z. J.; Colón, Y. J.; Siu, P. W.; Scheidt, K. A.; Snurr, R. Q.; Hupp, J. T.; Farha, O. K. A facile synthesis of UiO-66, UiO-67 and their derivatives. *Chem. Commun.* **2013**, *49* (82), 9449–9451. DOI: 10.1039/c3cc46105j

(39) Valenzano, L.; Civalleri, B.; Chavan, S.; Bordiga, S.; Nilsen, M. H.; Jakobsen, S.; Lillerud, K. P.; Lamberti, C. Disclosing the complex structure of UiO-66 metal organic framework: A synergic combination of experiment and theory. *Chem. Mater.* **2011**, *23* (7), 1700–1718. DOI: 10.1021/cm1022882

(40) Hernández Enríquez, J. M.; Cortez Lajas, L. A.; García Alamilla, R.; Castillo Mares, A.; Sandoval Robles, G.; García Serrano, L. A. Synthesis and characterization of mesoporous and nano-crystalline phosphate zirconium oxides. *J. Alloys Compd.* **2009**, *483* (1–2), 425–428. DOI: 10.1016/j.jallcom.2008.08.094

Table of Content

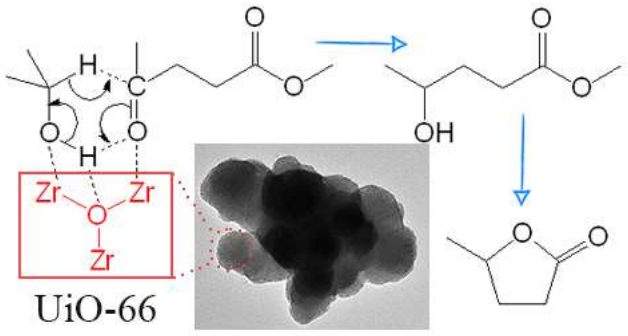

Unprecedented efficient and highly selective production of gamma valerolactone (58.9 to 92.3 $mmol_{gvl} \cdot g_{cat}^{-1} \cdot h^{-1}$) was achieved by UiO-66 catalyzed upgrading biomass-derived methyl levulinate in continuous flow process.